Coral Reefs (2017) 36:1291–1305
DOI 10.1007/s00338-017-1624-3

REPORT

Large-area imaging reveals biologically driven non-random spatial patterns of corals at a remote reef

Clinton B. Edwards[1] · Yoan Eynaud[1] · Gareth J. Williams[1,2] · Nicole E. Pedersen[1] · Brian J. Zgliczynski[1] · Arthur C. R. Gleason[3] · Jennifer E. Smith[1] · Stuart A. Sandin[1]

Received: 9 May 2016 / Accepted: 14 September 2017 / Published online: 12 October 2017

Abstract For sessile organisms such as reef-building corals, differences in the degree of dispersion of individuals across a landscape may result from important differences in life-history strategies or may reflect patterns of habitat availability. Descriptions of spatial patterns can thus be useful not only for the identification of key biological and physical mechanisms structuring an ecosystem, but also by providing the data necessary to generate and test ecological theory. Here, we used an in situ imaging technique to create large-area photomosaics of 16 plots at Palmyra Atoll, central Pacific, each covering 100 m^2 of benthic habitat. We mapped the location of 44,008 coral colonies and identified each to the lowest taxonomic level possible. Using metrics of spatial dispersion, we tested for departures from spatial randomness. We also used targeted model fitting to explore candidate processes leading to differences in spatial patterns among taxa. Most taxa were clustered and the degree of clustering varied by taxon. A small number of taxa did not significantly depart from randomness and none revealed evidence of spatial uniformity. Importantly, taxa that readily fragment or tolerate stress through partial mortality were more clustered. With little exception, clustering patterns were consistent with models of fragmentation and dispersal limitation. In some taxa, dispersion was linearly related to abundance, suggesting density dependence of spatial patterning. The spatial patterns of stony corals are non-random and reflect fundamental life-history characteristics of the taxa, suggesting that the reef landscape may, in many cases, have important elements of spatial predictability.

Keywords Coral reefs · Community structure · Landscape ecology · Spatial dispersion · Photomosaics · Palmyra Atoll

Communicated by Biology Editor Dr. Mark R. Patterson

Clinton B. Edwards and Yoan Eynaud contributed equally to this study.

Electronic supplementary material The online version of this article (doi:10.1007/s00338-017-1624-3) contains supplementary material, which is available to authorized users.

✉ Clinton B. Edwards
clint@ucsd.edu

[1] Center for Marine Biodiversity and Conservation, Scripps Institution of Oceanography, University of California, San Diego, La Jolla, CA 92093-0202, USA

[2] School of Ocean Sciences, Bangor University, Menai Bridge, Anglesey LL59 5AB, UK

[3] Physics Department, University of Miami, 1320 Campo Sano Ave, Coral Gables, FL 33146, USA

Introduction

The modern paradigm in coral reef ecology suggests that coral communities reflect a history of disturbance and subsequent decline (Bellwood et al. 2004). Despite this, some coral communities also reflect histories of remarkable survival and recovery following mortality events (Diaz-Pulido et al. 2009; Roff et al. 2014; Furby et al. 2017). The colonial growth form, for example, allows corals to sustain the loss of individual clones while maintaining overall colony function (Jackson and Coates 1986), and in some communities, fragmentation and colony regrowth can result in persistence of extremely long-lived corals (Highsmith et al. 1980; Edmunds 2015). The potential of colonies to shrink, grow and fragment is complemented by the fundamental importance of new colony creation through sexual reproduction that supports long-term population

genetic viability. Importantly, the breadth of demographic strategies within colonial corals, including recruitment, survival, fragmentation and recovery, provides a comparable breadth of spatial distribution processes. Investigation of spatial distributions in corals thus provides insights into the likely relative contribution of demographic mechanisms governing population dynamics across taxa.

The inferences that can be made through the study of spatial patterns at the scale of individual organisms have been of interest to geographers, naturalists and biologists for more than a century (Turner 1989). In the last 40 yr, renewed interest of terrestrial ecologists in spatial processes and patterns has led to the development of a suite of analytical tools to predict and describe spatial structure in nature (Wu 2013; Velázquez et al. 2016). To address spatial ecological questions, terrestrial landscape ecologists have taken advantage of comprehensive large-area sampling, often collected in the context of long-term study sites, including Barro Colorado Island (Hubbell and Foster 1992), the Hubbard Brook experimental forest (Bormann and Likens 2012) and various other locations (Condit et al. 2000). This work has identified a spectrum of dispersion patterns across ecosystems (Hubbell 1979; Lieberman et al. 1985; Condit et al. 2000) linked to a variety of key structuring mechanisms (e.g., recruitment patterns, habitat preference and availability, dispersal probabilities, resource limitation; Hubbell 1979; Connell 1985; Turner 1989; Condit et al. 2000; Rietkerk and van de Koppel 2008). Importantly, such work has been used to evaluate theoretical expectations of space use and to test candidate mechanisms generating the observed patterns, including the processes predicted by the Janzen–Connell hypothesis (Janzen 1970; Connell 1978) which has been shown to influence diversity in both tropical rainforests (Harms et al. 2000) and coral reefs (Marhaver et al. 2013).

To date, the study of spatial variability in coral communities has focused largely on site (Goreau 1959; Kenyon et al. 2010), reef/island (Newman et al. 2006; Sandin et al. 2008) or regional (Smith et al. 2016) patterns. Percentage cover data have formed the basis of this substantial body of work, with more limited efforts tracking spatial and demographic processes affecting individual colonies, such as fragmentation and partial survival (Hughes and Tanner 2000; Edmunds 2015). Importantly, such demographic insights require spatially explicit data at the level of the individual organism. Application of individual-level demographic data has been limited in subtidal marine environments largely due to the logistical constraints of obtaining data at the appropriate scale. Despite these difficulties, a number of studies have used individual-level data to study coral demography (Hughes 1984; Hughes and Tanner 2000; Edmunds 2015), to quantify competitive interactions (Bak et al. 1982; Bradbury and Young 1983; Reichelt and Bradbury 1984) or to describe habitat structure (Bak and Engel 1979; Bradbury and Young 1981), with comparably intense field campaigns tracking spatial disease patterns across populations (Jolles et al. 2002; Zvuloni et al. 2009). Less frequently collected are species-specific descriptions of spatial patterning of coral reef benthic organisms that rely on extremely labor-intensive in situ mapping (Lewis 1970; Stimson 1974; Dana 1976; Carlon and Olson 1993; Karlson et al. 2007; Deignan and Pawlik 2015). The value of such spatially explicit distribution data is clear, but the costs in terms of sub-tidal labor have limited the proliferation of these approaches in the broader marine scientific community.

Advances over the past decade in digital imaging, computing and data science now enable straightforward collection and creation of highly detailed composite large-area (hundreds to thousands of square meters) orthorectified photomosaics of sub-tidal benthic marine environments (Gracias et al. 2003; Lirman et al. 2007) (Fig. 1). Like other image-based underwater survey methods, such as video transects or photoquadrats, field-based image collections for photomosaics are complemented by laboratory-based data extraction. A variety of metrics, including percentage cover, species composition and disease or bleaching incidence, can be extracted from photomosaics using point counts, polygon digitization or other methods commonly used to analyze underwater imagery. Importantly, the high detail and large spatial extent of photomosaic surveys can capture thousands of individual coral colonies identifiable to species, enabling the extraction of spatially explicit information on benthic communities previously only available through intense field campaigns.

This study used a large-area imaging approach and spatial analysis to describe spatial patterns of coral communities at a remote Pacific atoll. Information from digitized photomosaics was used to enumerate and map individual corals in 16 plots representing 1600 m^2 of benthic habitat. We assessed the dispersion patterns of adult corals and investigated whether variability in measures of spatial dispersion was indicative of taxonomic differences or functional morphology. Further, we used targeted model fitting to test whether candidate habitat and biologically driven mechanisms might have generated the observed patterns. We also considered whether observed levels of dispersion were influenced by relative density of each group.

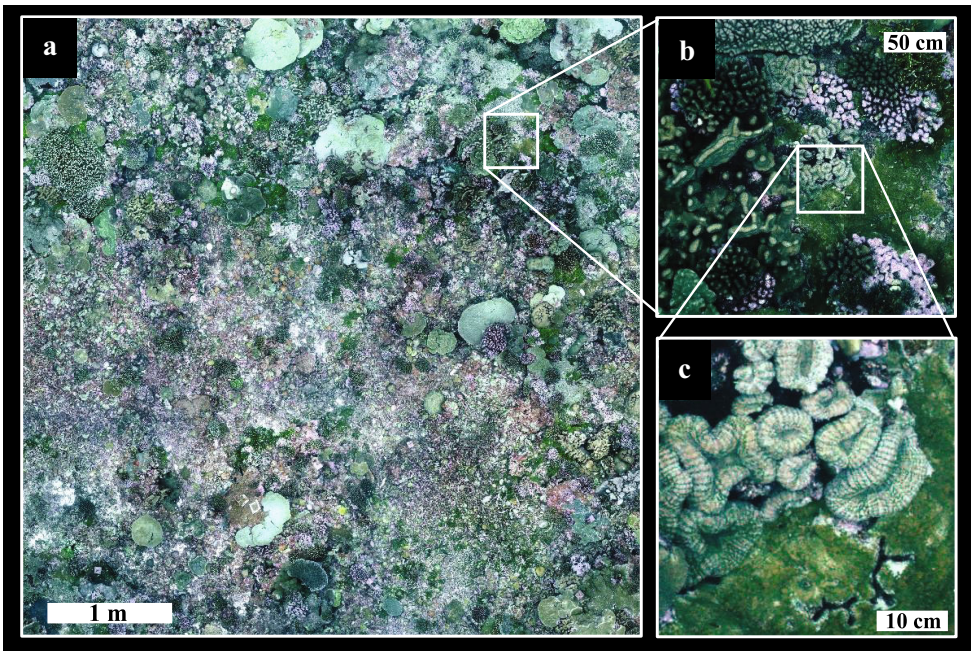

Fig. 1 **a** 25 m^2 subsection of raw landscape mosaic imagery and **b** embedded high-resolution composite images taken with the 55-mm focal length camera. The high-resolution imagery from the 55-mm camera enables detailed analysis of individual processes at small spatial scales **c** that can be mapped to the larger mosaic, allowing analyses to be conducted across scales. The image **b** is roughly commensurate in scale with imagery collected for standard point count percentage cover-based analyses. See electronic supplementary material Fig. S2 for full-size imagery

Methods

Study location

All work was conducted on Palmyra Atoll, a US Fish and Wildlife National Wildlife Refuge and part of the Pacific Remote Island Areas Marine National Monument, located approximately 1600 km south of Oahu, HI. Aside from alterations made to the lagoon (e.g., dredging and construction of causeways, docks and runways) during the brief military occupation in the mid-twentieth century, Palmyra's reef ecosystems have remained largely undisturbed by local human impacts (Sandin et al. 2008). In 2013, 16 plots were established on forereef habitats along the 10-m isobath and positioned for maximum spatial coverage across the atoll (Fig. 2).

Although photomosaics can be collected at a variety of spatial scales, for this study we analyzed imagery from 100 m^2 plots. Plots of this size were chosen as raw imagery can be collected easily during a single scuba dive and are manageable in the time-intensive step of ecological post-processing, while also capturing data at a sufficient scale to include thousands of coral colonies per plot (Table 1). All plots were established with two geo-referenced steel pins to facilitate repeat surveys.

Collection of mosaic imagery

Images for photomosaics were collected using two Nikon D7000 16.2 megapixel DSLR still cameras mounted to a custom frame. The camera used to generate processed photomosaics was equipped with a wide-angle 18-mm focal length lens to ensure high overlap between adjacent images. The second camera was equipped with a 55-mm focal length lens to capture images with $\leq$ 1 mm resolution. To obtain continuous coverage of the reef floor within a plot, the diver operating the camera system swam a gridded pattern approximately 1.5 m above the average depth of the plot at speeds (5–7 m min^{-1}) sufficient to maintain maximum overlap between adjacent images. Images were captured every second from each still camera using the built-in intervalometers. Depending on conditions, a single mosaic could be collected in 45–60 min and consisted of approximately 2500 individual images per still camera.

Technical processing of mosaic imagery

The details of the technical processing software used to generate the photomosaics have been described previously (Gracias et al. 2003; Lirman et al. 2007). Briefly, photomosaics are created from raw images using image processing and numerical optimization modules that work with little user intervention. The output is an orthorectified photomosaic generated by fusing the registered images together. Measurements collected in the field between ground control points (electronic supplementary material, ESM, Fig. S1) are used to calibrate the composite rendering.

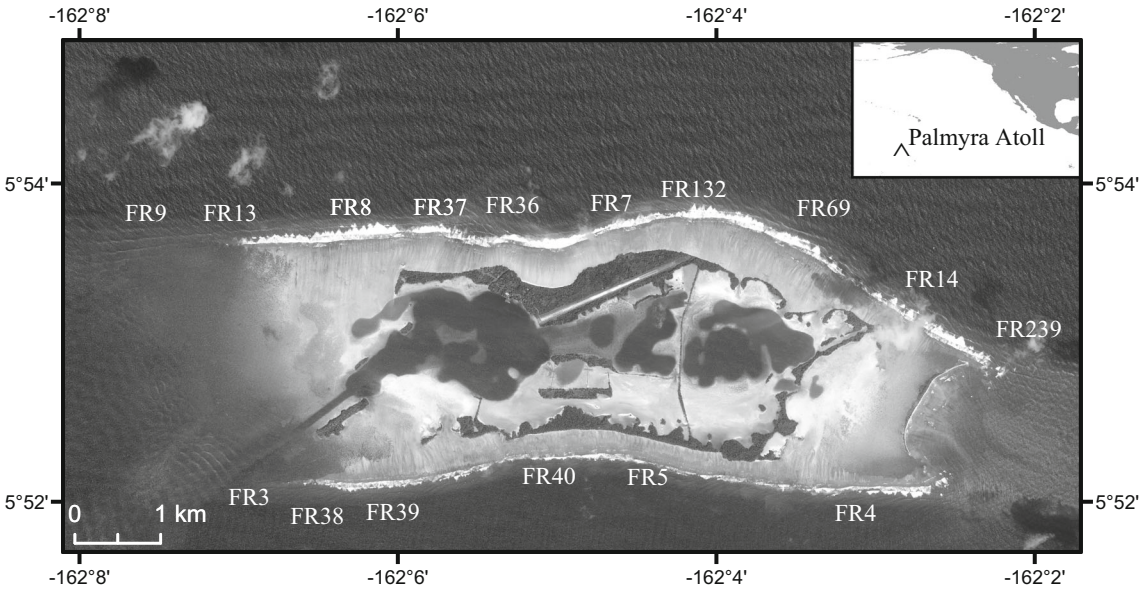

Fig. 2 Satellite image of the location of study plots at Palmyra Atoll, a remote uninhabited atoll and National Wildlife Refuge located approx. 1600 km south of the Hawaiian Islands (inset)

Ecological post-processing of mosaic imagery

Photomosaics were post-processed through a manual digitization process adapted from previous work (Lirman et al. 2007). Mosaic images were first uploaded to Adobe Photoshop CC, and the boundaries of all corals > 9 cm^2 were digitized by hand using a Wacom pen-tablet (model # CTH-470). Linked high-resolution imagery was used to separate adjacent colonies of the same species (Fig. 1). We followed the operational definition of a colony as a contiguous patch of live tissue (Highsmith 1982). Using the best available species lists (ESM Table S1), we designated corals to the highest taxonomic level possible. When the species could not be determined, taxa were grouped within genera based on functional morphology (ESM Table S1). To determine whether spatial patterns also varied at the functional level, corals were grouped by functional morphology. Corals were classified as branching, corymbose, encrusting, free-living, massive, plating, sub-massive or tabular using the best available sources (ESM Table S1). Taxonomic and functional morphology designations were confirmed with high-resolution imagery (Fig. 1). Different taxonomic groups were then represented as separate image 'layers' in Photoshop and exported as individual PNG image files.

Analytical processing of mosaic imagery

Exported image files were processed analytically using custom algorithms designed by the authors using R 3.2 (R Core Team 2016). The algorithm reads RGB pixel values from the individual digitized PNG image files to identify and enumerate individual coral colonies and calculate percentage cover/surface area. Distance between ground control points (in cm) was measured in the field (ESM Fig. S1) and compared to the distances in the photomosaics (in pixels) to establish the ratio of pixels to cm scale and to internally georeference and calibrate photomosaics, in turn creating a spatially explicit map of each plot. Previous evaluations of geometric accuracy in photomosaic imagery have shown maximum distance errors ranging from 10.7 to 13.5 cm, while evaluations of abundance, diversity and percentage cover were statistically indistinguishable from standard methodologies (Lirman et al. 2007). The count-based metrics used here are robust to distance errors, especially with large sample sizes. However, we performed a sensitivity analysis to evaluate potential bias in abundance estimates. Drawing from a normal probability distribution of offset values ranging from 0 to the maximum error distance, we randomly assigned coral colonies' spatial offset values and found no significant difference in abundance or aggregation metrics.

Quantitative processing of mosaic imagery

After corals were enumerated and mapped in each photomosaic (ESM Fig. S2a–p), we described the spatial patterns of corals at the finest taxonomic resolution possible to determine how individual species or taxonomic groups of corals drive the observed patterns. We then quantified patterns using a functional morphology-based approach to

explore how shared morphological and life-history strategies might contribute to common spatial patterning.

Dispersion patterns

One of the oldest and most frequently applied measures of spatial patterning, the variance-to-mean ratio (VMR) (Dale 1999; Dale et al. 2002) allows identification of departures from complete spatial randomness (CSR); potential alternatives are increased uniformity (i.e., individuals more evenly spaced than expected) or increased clustering (i.e., individuals more aggregated than expected) (sensu Hutchinson 1953; Dale 1999).

Our calculation of VMR used a simulated quadrat sampling approach commensurate in scale to the imagery collected by most benthic monitoring and research programs. Using a bootstrapping approach, we estimated the mean and variation of VMR across each of the 16 plots for each of the taxonomic and functional morphological groups. For each group, i, and each plot, j, we sampled $Q = 25$ non-overlapping 1-m^2 quadrats and counted all colony centroids in each quadrat, n_q. We then calculated the mean ($\mu_{i,j,k}$) and VMR ($v_{i,j,k}$) of the number of colony centroids from the $N = 25$ quadrats for each bootstrapped replicate, k. Summary statistics were calculated as follows:

$$v_{i,j,k} = \frac{\sigma^2_{i,j,k}}{\mu_{i,j,k}} \quad \text{with } \mu_{i,j,k} = \frac{1}{Q}\sum_{q=1}^{Q} n_{i,j,k,q} \quad \text{and}$$

$$\sigma^2_{i,j,k} = \frac{1}{Q}\sum_{q=1}^{Q}\left(n_{i,j,k,q} - \mu_{i,j,k}\right)^2$$

By repeating this process B times for each plot, setting $B = 1000$, we obtained a distribution of VMR values for each taxonomic and functional morphological group composing the set, $\left(v_{i,j,1}, \ldots, v_{i,j,k}, \ldots, v_{i,j,B}\right)$. Next, we calculated the mean VMR for each replicate (k) across the j plots to obtain a distribution of means, $\left(\bar{v}_{i,1}, \ldots, \bar{v}_{i,k}, \ldots, \bar{v}_{i,B}\right)$ for each group, expressed as:

$$\bar{v}_{i,k} = \frac{1}{M}\sum_{j=1}^{M} v_{i,j,k}$$

where M is the total number of plots. From this distribution, we then estimated the bootstrapped mean VMR for each group:

$$\bar{\bar{v}}_i = \frac{1}{B}\sum_{k=1}^{B} \bar{v}_{i,k}$$

Finally, we estimated the 95% confidence interval of this distribution, $\bar{\bar{v}}_{i,0.025}$ and $\bar{\bar{v}}_{i,0.975}$ for each group i, where $\bar{\bar{v}}_{i,\alpha}$ is the α^{th} quartile of the vector of bootstrapped mean VMRs for each i. For values of $\bar{\bar{v}}_{i,0.025} > 1$, the dispersion pattern is clustered, if $\bar{\bar{v}}_{i,0.025} < 1$ and $\bar{\bar{v}}_{i,0.975} > 1$, the dispersion pattern is random and when $\bar{\bar{v}}_{i,0.975} < 1$, the spatial distribution is over-dispersed.

Model comparison

To explore potential processes contributing to the observed spatial patterns, we used a goodness-of-fit approach to compare four hypothesized null models of spatial patterning for each group, as follows: (1) a homogeneous Poisson process, where all points (e.g., colony centroids) are randomly and independently distributed across the landscape (e.g., CSR) and which is analogous to the VMR approach; (2) a non-homogeneous Poisson (NHP) process which models patterns created by availability of open space or habitat preferences, defined here as habitat filtering; (3) a homogeneous clustering process (HC) which represents biotic mechanisms such as spatially constrained dispersal and fragmentation; and (4) a non-homogeneous clustering (NHC) process which combines both habitat filtering and biotic clustering and processes.

For each taxonomic and functional morphology group in each plot, we used a simulation procedure to compare the observed spatial patterns against each of the null models outlined above using the pair correlation function (PCF), a non-cumulative second-order summary statistic (Baddeley et al. 2015). The PCF represents the expected density of colony centroids within rings of radius r centered on the centroid of the focal colony divided by the intensity of the spatial pattern. We then compared the difference between the mean values from the simulations and the observed values for each group, allowing us to test the fit of the null hypothesis that the observed pattern was similar to the model it was tested against. Note that the analyses were conducted only on those groups with sufficient statistical power, defined here as groups with at least 20 colonies present in at least four plots, i.e., 25% of our plots.

For a detailed explanation of the model comparison approach, please see ESM Methods 1: Model comparison and references therein.

Density dependence

To identify potential density dependence in the observed levels of dispersion, we used linear regression to describe relationships between the colony density (number 100 m^{-2}) and the mean VMR value of each bootstrapped sample at each plot for each group, expressed as:

$$\bar{v}_{i,j} = \frac{1}{B}\sum_{k=1}^{B} v_{i,j,k}.$$

For many groups, there was a large range in colony density across plots; hence, colony density data and mean VMR values, $\bar{v}_{i,j}$, were log transformed for all groups. Regressions were conducted for both taxonomic and functional morphology analyses.

To maximize the power of the VMR and linear regression analyses, we only considered groups with at least ten colonies present in at least four plots (25% of our sample). Further, plots with less than ten colonies for a given group were dropped from the analysis as this is the minimum number of colonies required to make inferences about dispersion patterns.

Development of models and all analyses were completed using R 3.2, and the package *spatstat* was used for the model comparison section (R Core Team 2016).

Results

Abundance and percentage cover patterns

We identified 44,008 individual coral colonies (> 9 cm^2) from 33 different taxonomic groups (ESM Table S1) belonging to eight functional morphology groups in 1600 m^2 of forereef habitat (16 plots, each 100 m^2) (Table 1; ESM Fig. S2a–p). Abundance ranged from a maximum of 4980 coral colonies 100 m^{-2} to a minimum of 1572 colonies 100 m^{-2} with an average of 2750 ± 256 (SE) colonies 100 m^{-2} across all 16 plots (Table 1). The number of colonies per taxonomic and functional group was variable between plots. *Porites superfusa* was the most abundant taxonomic group in nine of the 16 plots, with an average of 696 ± 108 colonies 100 m^{-2}. The next most abundant group, the genus *Fungia,* was nearly half as abundant, with 383 ± 131 colonies 100 m^{-2}. However, *Fungia* also displayed the highest variability, with abundance ranging from 22 to 1752 colonies 100 m^{-2}, and had the highest single plot abundance. The third most abundant group, the genus *Pocillopora*, demonstrated much less variability across plots with abundance ranging from 166 to 565 colonies 100 m^{-2} with an average of 330 ± 26 colonies 100 m^{-2}. At the other end of the spectrum, nine of 33 observed taxonomic groups were represented by fewer than 100 colonies across all 16 plots (Table 1).

Coral cover ranged from 12.0 (Table 2) to 31.3%, with an average of 22.7 ± 1.3%. As with numerical abundance, percentage cover of the various taxonomic and functional groups was variable among plots. Massive corals of the genus *Porites* had the highest percentage cover in eight of 16 plots, with an average cover of 3.8 ± 0.5% across the 16 plots. The group with the second highest mean percentage cover, *Pocillopora* (3.3 ± 0.3%), was also the third most numerically abundant group. The group with the third highest mean percentage cover, encrusting *Montipora*, demonstrated the greatest variability across plots with percentage cover ranging from 0.7 to 8.0%; it was also the group with the highest single plot percentage cover (Table 2).

Dispersion patterns

Of the 32 taxonomic groups in the 16 plots, 23 had sufficient sample sizes to investigate dispersion patterns, while all eight functional morphologies had sufficient sample sizes for the analysis. Overall, we found that adult hard corals were highly clustered grouped by both taxonomy and functional morphology (Fig. 3a, b), with little or no evidence for randomness or uniformity.

The degree of dispersion was variable within and among taxonomic groups, but there was a strong tendency for clustering. We found evidence (i.e., $\bar{\bar{v}}_{i,0.025} > 1$) of spatial clustering in 21 of the 23 coral groups considered (Fig. 3b). Corals of the genus *Fungia* displayed the greatest median VMR as well as the greatest variability across the 16 plots. Other groups with high levels of clustering (branching *Acropora*, *Favia stelligera* and *Turbinaria reniformis*) also showed similar levels of variability. *Porites superfusa*, on the other hand, displayed the second highest median VMR, but with much lower variability than other highly clustered groups. Although still significantly clustered, the lowest levels of VMR were found in sub-massive corals of the genus *Favites* and the fast-growing table *Acropora* and corymbose *Pocillopora* groups. We found nonsignificant departures from randomness (i.e., $\bar{\bar{v}}_{i,0.025} < 1$ and $\bar{\bar{v}}_{i,0.975} > 1$) in only two groups of corals, massive colonies of the genus *Platygyra* and the species *Pocillopora eydouxi* (Fig. 3b).

There was also variability in the level of spatial dispersion among functional morphology groups. Despite this variability, all eight of the observed functional morphology groups showed clustered dispersion patterns (Fig. 3a). Overall, the free-living morphology showed the greatest degree of clustering. These results strongly reflect the pattern of the numerically dominant genus *Fungia*, as other free-living groups were rare. Other morphologies exhibiting high levels of clustering were the encrusting and branching morphologies. As the branching morphology was comprised of only a single taxonomic group (*Acropora*), caution should be used in generalizing the results.

Model comparison

Results of the null model comparisons show striking patterns of non-randomness; the CSR model (model 1) was

Table 1 Total number of coral colonies in 32 taxonomic and eight functional morphology groups at each of 16 sites at Palmyra Atoll (sites are arranged counterclockwise starting with FR3; Fig. 2)

Group	Morphology	FR3	FR38	FR39	FR40	FR5	FR4	FR239	FR14	FR69	FR132	FR7	FR36	FR8	FR37	FR13	FR9	Total
Acropora sp.	Branching	0	161	18	73	0	0	0	49	0	3	0	71	0	11	0	0	386
Acropora sp.	Corymbose	0	35	5	36	1	11	66	2	5	10	1	11	1	9	2	25	220
Pocillopora eydouxi	–	4	4	11	13	0	0	12	8	10	27	0	11	0	29	29	0	158
Pocillopora sp.	–	244	457	277	290	450	406	365	166	239	359	236	309	219	372	329	565	5283
Stylophora pistillata	–	82	0	0	6	72	167	0	0	0	0	4	0	0	0	122	390	843
Group total	–	330	496	293	345	523	584	443	176	254	396	241	331	220	410	482	980	6504
Favites sp.	Encrusting	18	48	49	59	9	21	23	51	35	118	47	85	59	125	119	0	866
Leptastrea sp.	–	0	32	17	71	0	0	7	8	6	86	9	13	27	25	10	6	317
Leptoseris sp.	–	0	1	0	5	0	4	2	5	3	3	0	4	0	3	5	0	35
Montipora sp.	–	100	328	114	260	58	103	175	43	46	251	64	397	217	284	124	132	2696
Pasmmocora sp.	–	1	1	0	1	0	0	5	7	4	5	0	1	0	0	13	0	38
Pavona varians	–	125	132	102	230	42	141	91	93	64	354	103	156	110	102	174	77	2096
Porites superfusa	–	529	849	557	406	320	1760	878	501	959	443	198	347	270	939	1449	726	11,131
Group total	–	773	1391	836	1032	429	2029	1181	708	1117	1260	421	1003	683	1478	1894	941	17,179
Fungia sp.	Free-living	1032	68	83	57	360	1112	119	68	61	37	176	22	47	200	1752	940	6134
Halomitra pileus	–	0	0	0	0	0	0	0	0	0	0	0	0	0	0	12	0	12
Herpolitha sp.	–	0	0	0	1	0	0	0	2	0	1	0	0	0	0	0	0	4
Sandalolitha dentata	–	0	1	1	0	0	0	0	0	0	0	0	0	0	0	0	0	2
Group total	–	1032	69	84	58	360	1112	119	70	61	38	176	22	47	200	1764	940	6152
Favia matthai	Massive	0	1	2	2	0	239	1	1	0	7	0	0	0	0	1	95	349
Hydnophora microconos	–	16	151	131	178	0	12	68	39	42	217	57	184	125	182	14	21	1437
Lobophyllia sp.	–	16	0	0	0	257	7	0	0	0	0	4	0	0	2	68	54	408
Montastrea curta	–	12	85	55	128	0	20	132	128	113	452	51	332	169	345	35	19	2076
Platygyra sp.	–	9	20	11	17	2	2	6	24	7	53	14	40	26	13	7	11	262
Porites rus	–	0	0	0	1	0	0	0	0	0	0	0	0	0	7	0	0	8
Porites sp.	–	88	217	164	203	66	92	200	162	85	336	242	182	148	280	95	70	2630
Group total	–	141	474	363	529	325	372	407	354	247	1065	368	738	468	829	220	270	7170
Hydnophora exesa	Plating	26	4	1	0	3	12	13	1	0	0	0	0	3	14	12	23	112
Montipora sp.	–	10	65	64	59	1	16	2	9	1	11	0	88	49	70	67	3	515
Turbinaria reniformis	–	0	42	167	0	0	0	99	1	137	175	127	90	126	85	124	317	1490
Group total	–	36	111	232	59	4	28	114	11	138	186	127	178	178	169	203	343	2117
Astreopora myriophthalma	Sub-massive	0	0	1	0	0	0	0	0	0	0	3	1	0	0	0	0	5
Favia stelligera	–	118	310	244	188	20	0	160	134	84	174	127	187	0	198	89	0	2033
Favites sp.	–	7	21	32	53	0	20	12	7	2	18	38	14	31	20	5	0	280
Gardineroseris planulata	–	0	0	0	0	1	0	0	0	0	0	0	0	0	0	0	0	1
Goniastrea pectinata	–	0	0	0	5	0	0	1	0	1	2	0	0	0	0	0	0	9
Pavona sp.	–	79	58	65	101	13	474	88	99	62	179	71	104	247	103	307	17	2067
Group total	–	204	389	342	347	33	494	261	240	149	373	239	306	278	321	401	17	4394
Acropora sp.	Tabular	12	10	1	15	0	2	2	0	4	13	0	7	12	10	16	1	105
Total	All	2528	3101	2172	2458	1674	4621	2527	1608	1970	3334	1572	2656	1886	3428	4980	3492	44,008

Table 2 Percentage cover (percentage of benthic substrate 100 m^{-2}) of taxonomic and functional morphology groups at each of 16 sites at Palmyra Atoll (sites are arranged counterclockwise starting with FR3; Fig. 2)

Group	Morphology	FR3	FR38	FR39	FR40	FR5	FR4	FR239	FR14	FR69	FR132	FR7	FR36	FR8	FR37	FR13	FR9	Average
Acropora sp. (branching)	Branching	0.0	3.8	0.4	0.6	0.0	0.0	0.0	1.2	0.0	0.1	0.0	0.9	0.0	0.3	0.0	0.0	0.4
Acropora sp. (corymbose)	Corymbose	0.0	0.2	0.0	0.6	0.0	0.1	0.9	0.2	0.1	0.0	0.0	0.1	0.1	0.1	0.0	0.2	0.2
Pocillopora eydouxi	–	0.1	0.0	0.1	0.3	0.0	0.0	0.3	0.3	0.3	0.7	0.0	0.3	0.0	1.0	0.4	0.0	0.2
Pocillopora sp.	–	3.4	3.5	3.1	2.7	4.4	3.1	3.5	1.9	2.9	3.2	3.0	2.5	2.8	3.7	2.6	6.7	3.3
Stylophora pistillata	–	1.1	0.0	0.0	0.0	0.9	1.8	0.0	0.0	0.0	0.0	0.0	0.0	0.0	0.0	1.1	5.9	0.7
Group total	–	4.5	3.7	3.3	3.7	5.3	5.0	4.7	2.3	3.2	3.9	3.0	2.9	2.9	4.7	4.0	12.8	4.4
Favites sp. (encrusting)	Encrusting	0.4	0.2	0.3	0.3	0.1	0.2	0.1	0.3	0.2	1.0	0.3	0.5	0.3	0.8	0.6	0.0	0.3
Leptastrea sp.	–	0.0	0.2	0.1	0.5	0.0	0.0	0.0	0.1	0.0	0.6	0.1	0.1	0.2	0.1	0.1	0.1	0.1
Leptoseris sp.	–	0.0	0.0	0.0	0.0	0.0	0.0	0.0	0.0	0.0	0.0	0.0	0.0	0.0	0.0	0.0	0.0	0.0
Montipora sp. (encrusting)	–	3.7	5.1	1.9	3.2	1.1	1.6	2.9	0.8	1.0	2.9	0.7	8.0	3.2	3.8	2.1	3.5	2.8
Pasmmocora sp.	–	0.0	0.0	0.0	0.0	0.0	0.0	0.1	0.1	0.0	0.0	0.0	0.0	0.0	0.0	0.1	0.0	0.0
Pavona varians	–	0.6	0.6	0.6	1.3	0.3	0.6	0.7	0.6	0.3	1.8	0.5	0.5	0.5	0.4	0.4	0.3	0.6
Porites superfusa	–	1.2	1.4	1.1	0.6	1.0	3.1	3.2	1.5	2.4	0.6	0.4	0.7	0.4	1.9	2.7	2.4	1.5
Group total	–	5.9	7.4	4.0	5.9	2.4	5.4	6.9	3.4	3.9	6.9	2.0	9.6	4.6	7.0	5.8	6.3	5.5
Fungia sp.	Free-living	3.9	0.2	0.3	0.2	0.8	1.9	0.4	0.2	0.1	0.1	0.6	0.0	0.1	0.2	2.6	3.4	0.9
Halomitra pileus	–	0.0	0.0	0.0	0.0	0.0	0.0	0.0	0.0	0.0	0.0	0.0	0.0	0.0	0.0	0.2	0.0	0.0
Herpolitha sp.	–	0.0	0.0	0.0	0.0	0.0	0.0	0.0	0.0	0.0	0.0	0.0	0.0	0.0	0.0	0.0	0.0	0.0
Sandalolitha dentata	–	0.0	0.1	0.0	0.0	0.0	0.0	0.0	0.0	0.0	0.0	0.0	0.0	0.0	0.0	0.0	0.0	0.0
Group total	–	3.9	0.2	0.3	0.2	0.8	1.9	0.4	0.2	0.1	0.1	0.6	0.0	0.1	0.2	2.8	3.4	1.0
Favia matthai	Massive	0.0	0.1	0.3	0.1	0.0	4.2	0.0	0.0	0.0	0.2	0.0	0.0	0.0	0.0	0.1	1.8	0.4
Hydnophora microconos	–	0.6	0.8	1.5	1.5	0.0	0.3	0.5	0.4	0.5	1.9	1.0	2.0	2.0	2.0	0.3	0.4	1.0
Lobophyllia sp.	–	1.3	0.0	0.0	0.0	5.6	0.1	0.0	0.0	0.0	0.0	0.0	0.0	0.0	0.0	0.6	0.7	0.5
Montastrea curta	–	0.1	0.3	0.4	0.7	0.0	0.1	0.5	0.7	0.6	1.7	0.3	1.2	1.0	1.7	0.2	0.1	0.6
Platygyra sp.	–	0.2	0.1	0.1	0.2	0.2	0.1	0.1	0.2	0.1	0.6	0.2	0.4	0.3	0.2	0.1	0.5	0.2
Porites rus	–	0.0	0.0	0.0	0.0	0.0	0.0	0.0	0.0	0.0	0.0	0.0	0.0	0.0	0.2	0.0	0.0	0.0
Porites sp. (massive)	–	7.8	5.0	5.5	3.3	1.2	3.2	3.9	5.0	1.4	4.4	6.5	3.0	3.2	4.3	2.2	1.4	3.8
Group total	–	10.0	6.3	7.8	5.8	6.9	8.0	5.0	6.3	2.6	8.8	7.9	6.6	6.4	8.3	3.4	4.9	6.6
Hydnophora exesa	Plating	1.4	0.1	0.0	0.0	0.0	0.2	0.3	0.0	0.0	0.0	0.0	0.0	0.2	0.3	0.3	0.6	0.2
Montipora sp. (plating)	–	0.7	1.6	2.5	1.5	0.0	0.7	0.0	0.3	0.0	0.4	0.0	2.7	1.6	2.7	1.8	0.3	1.0
Turbinaria reniformis	–	0.0	0.4	1.9	0.0	0.0	0.0	0.5	0.0	0.9	0.9	1.4	0.6	2.1	0.3	0.3	2.2	0.7
Group total	–	2.1	2.1	4.4	1.5	0.0	0.9	0.9	0.3	0.9	1.2	1.4	3.4	3.8	3.3	2.4	3.1	2.0
Astreopora myriophthalma	Sub-massive	0.0	0.0	0.3	0.0	0.0	0.0	0.0	0.0	0.0	0.0	0.3	0.0	0.0	0.0	0.0	0.0	0.0
Favia stelligera	–	3.2	1.3	2.9	1.5	0.6	0.0	0.9	1.1	0.8	1.9	1.4	1.6	0.0	2.1	1.2	0.0	1.3
Favites sp. (sub-massive)	–	0.5	0.1	0.5	1.0	0.0	0.4	0.3	0.2	0.0	0.2	0.7	0.1	0.5	0.3	0.1	0.0	0.3
Gardineroseris planulata	–	0.0	0.0	0.0	0.0	0.0	0.0	0.0	0.0	0.0	0.0	0.0	0.0	0.0	0.0	0.0	0.0	0.0
Goniastrea pectinata	–	0.0	0.0	0.0	0.0	0.0	0.0	0.0	0.0	0.0	0.0	0.0	0.0	0.0	0.0	0.0	0.0	0.0
Pavona sp. (sub-massive)	–	0.8	0.6	0.5	0.9	0.1	2.3	0.6	0.9	0.4	1.4	0.7	0.9	2.4	0.6	1.4	0.2	0.9
Group total	–	4.6	2.1	4.2	3.4	0.7	2.7	1.9	2.1	1.2	3.5	3.1	2.7	3.0	3.0	2.7	0.2	2.6
Acropora sp. (tabular)	Tabular	0.3	2.0	0.1	1.0	0.0	0.0	0.1	0.0	0.2	0.2	0.0	0.3	0.6	0.2	1.3	0.0	0.4
Total		31.3	27.5	24.4	22.0	16.2	23.7	19.8	15.8	12.0	24.8	17.9	26.5	21.3	27.0	22.4	30.7	22.7

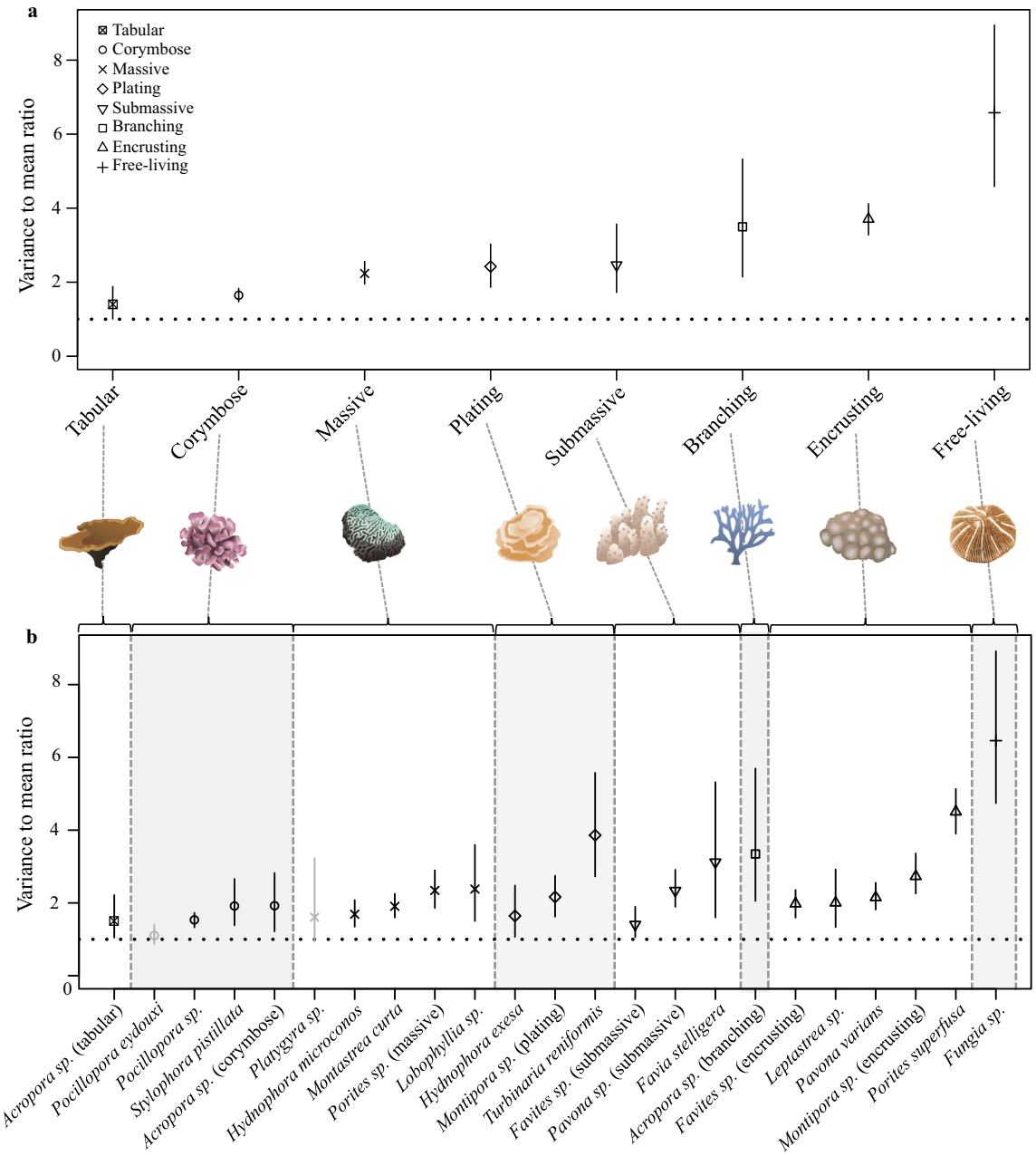

Fig. 3 Dispersion results by **a** functional group and **b** species. Boxplots of simulated VMR distributions show medians (symbols) and 95% quantile ranges (lines) of the bootstrapped VMR distributions. The dotted line indicates VMR = 1 (randomness), and 95% quantile ranges not overlapping 1 are indicative of significant departures from randomness

rejected for all observed taxonomic and functional morphology groups (Fig. 4). These results are consistent with the VMR analysis, with two notable differences: *Pocillopora eydouxi* did not significantly depart from randomness in the VMR analysis despite rejection from model 1; and *Platygyra* sp. was not included in model comparisons due to limited sample sizes. The goodness-of-fit for NHP model (model 2) was rejected for all but four of the 22 taxonomic groups examined: branching and corymbose *Acropora* species, *Hydnophora exesa* and *Pocillopora eydouxi.* The only functional morphology group comparison for which the NHP model could not be rejected was the branching corals (Fig. 4). Given that this group is made up exclusively of branching *Acropora* species, these results are unsurprising.

We found little support to reject the clustering models (either model 3 or 4) as an underlying cause leading to the observed distributions for the taxa examined (Fig. 4). Both

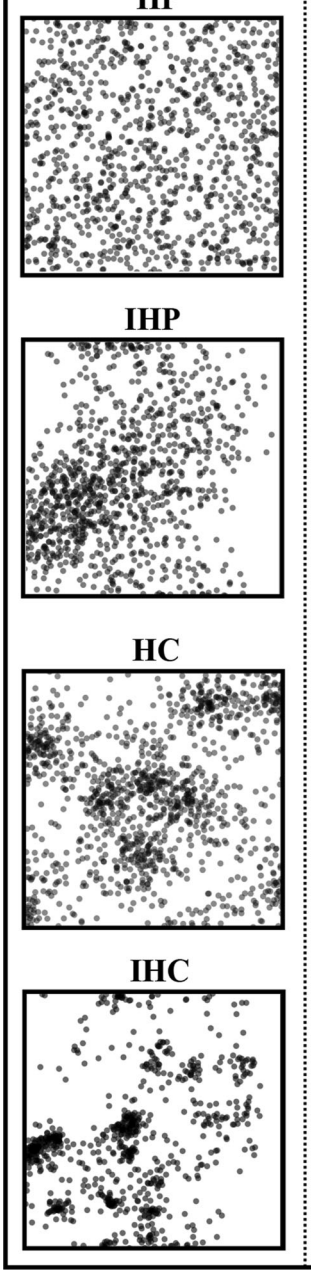

b

Group	Supported models
Branching	IHP, HC, IHC
Corymbose	HC, IHC
Encrusting	IHC
Free-living	HC, IHC
Massive	HC, IHC
Plating	HC, IHC
Sub-massive	-
Acropora sp. (branching)	IHP, HC, IHC
Acropora sp. (corymbose)	IHP, HC, IHC
Favia matthai	HC, IHC
Favia stelligera	-
Favites sp. (encrusting)	HC, IHC
Favites sp. (submassive)	HC
Fungia sp.	HC, IHC
Hydnophora exesa	IHP, HC, IHC
Hydnophora microconos	-
Leptastrea sp.	HC, IHC
Lobophyllia sp.	HC, IHC
Montastrea curta	HC, IHC
Montipora sp. (encrusting)	IHC
Montipora sp. (plating)	HC, IHC
Pavona sp. (submassive)	HC, IHC
Pavona varians	IHC
Pocillopora sp.	IHC
Pocillopora eydouxi	HC
Porites sp. (massive)	HC,IHC
Porites superfusa	IHC
Stylophora pistillata	HC
Turbinaria reniformis	HC, IHC

Fig. 4 **a** Stereotypical examples of each of four simulated distributions: (1) homogeneous Poisson (HP); (2) non-homogeneous Poisson (NHP); (3) homogeneous clustering process (HC); and (4) non-homogeneous clustering process (NHC). **b** Model comparison results by functional and taxonomic group for each of the simulated null models of spatial dispersion showing only the models fitting each group. As the HP model did not fit any of the groups it has been omitted; groups with no model fits are designated with a dash

clustering models were rejected for only two coral species, *Hydnophora microconos* and *Favia stelligera*. We did not find evidence to reject HC model (model 3) for *Favites* sp. (sub-massive) *Pocillopora eydouxi* or *Stylophora pistillata*, but there was support to reject NHC model (model 4) for these three groups. On the other hand, while we rejected the HC model for *Montipora* sp. (encrusting), *Pocillopora* sp. and *Porites superfusa,* we did not find support to reject the NHC model for these groups (Fig. 4).

In the functional group comparisons, both clustering models (models 3 and 4) were rejected only for sub-massive corals. However, as this group is numerically dominated by *Favia stelligera* (46% of colonies), generalization of these results should be done with caution. Similarly, we rejected the HC model (model 3) for encrusting corals; however, this group is heavily dominated by *Porites superfusa* (65% of colonies) for which the HC model was also rejected.

Density dependence

While only a limited number of groups showed significant relationships, there was an overall tendency for positive density dependence in VMR values (Table 3). Of the 23 groups with adequate sample sizes, only *Fungia*, encrusting *Montipora*, *Pocillopora* and *Porites superfusa* showed significant positive relationships in the linear regressions between colony abundance and the VMR (Table 3). While the free-living, corymbose and encrusting functional morphologies showed significant density dependence, these results reflect the influence of the hyper-abundant *Fungia*, *Pocillopora* and *Porites superfusa* groups.

We did not observe any negative relationships between colony abundance and the VMR. Across all groups, the lack of density dependence did not appear to be related to truncated abundance ranges, as many coral groups showing non-significant relationships between abundance and VMR exhibited large differences in colony abundance across the 16 plots (Tables 1, 3).

Table 3 Results of linear regressions of variance-to-mean ratio and colony abundance for 23 taxonomic and eight functional groups

Group	Morphology	β	R^2	p	n
Acropora	Branching	0.12	0.07	0.61	6.00
Acropora	Corymbose	0.36	0.41	0.12	7.00
**Pocillopora*	–	0.32	0.29	0.03	16.00
Pocillopora eydouxi	–	0.01	0.00	0.93	8.00
Stylophora pistillata	–	0.26	0.16	0.51	5.00
*Group total	–	0.41	0.67	0.00	16.00
Favites	Encrusting	0.17	0.19	0.12	14.00
Leptastrea	–	0.15	0.20	0.27	8.00
**Montipora*	–	0.23	0.31	0.03	16.00
Pavona varians	–	0.09	0.03	0.51	16.00
**Porites superfusa*	–	0.49	0.68	0.00	16.00
*Group total	–	0.76	0.48	0.00	16.00
**Fungia*	Free-living	0.65	0.74	0.00	16.00
Favia stelligera	Massive	0.24	0.06	0.43	13.00
Hydnophora microconos	–	0.05	0.06	0.38	15.00
Lobophyllia	–	0.32	0.67	0.18	4.00
Montastrea curta	–	0.08	0.10	0.27	15.00
Platygyra	–	0.01	0.00	0.97	10.00
Porites	–	-0.20	0.12	0.18	16.00
Group total	–	-0.04	0.01	0.73	16.00
Hydnophora exesa	Plating	-0.01	0.00	0.99	6.00
**Montipora*	–	0.36	0.88	0.00	10.00
Turbinaria reniformis	–	0.12	0.02	0.71	11.00
Group total	–	0.15	0.10	0.26	15.00
Favites	Sub-massive	0.16	0.10	0.37	10.00
Pavona	–	0.16	0.17	0.11	16.00
Group total	–	0.18	0.02	0.58	16.00
Acropora	Tabular	0.78	0.30	0.20	7.00

Significant relationships indicated by *asterisks*, n is the number of plots with sufficient abundance for analysis (> 10 colonies per plot)

Discussion

We described the spatial distribution of scleractinian corals across 16 plots at the remote coral reef, Palmyra Atoll, using methodological and quantitative approaches developed to address spatial ecological questions in terrestrial systems. In our exploration of spatial dispersion, we found an overall tendency for individual corals within taxonomic groups to be clustered across the landscape, but the degree to which they aggregated varied by taxon. Similarly, functional morphology groups also had clustered distributions. Next, using a goodness-of-fit model fitting procedure, we explored whether the observed spatial distributions matched simulated distributions based on hypothesized mechanisms of habitat filtering and biotic clustering processes such as dispersal limitation and fragmentation. We did not find support for the random spatial (i.e., CSR) model in any of the observed functional or taxonomic groups. Overwhelmingly, our observed distributions were most consistent with models of biotic clustering (models 3 and 4), with little support for habitat filtering (model 2) alone as a putative mechanism for the observed patterns. While levels of clustering were variable within taxonomic and functional groups, we found an overall tendency for the degree of clustering to be positively related to abundance.

Previous work investigating spatial patterns in corals has found similar, but more equivocal, results (Lewis 1970; Carlon and Olson 1993; Karlson et al. 2007). Similarly, there are a range of dispersion patterns in terrestrial plant communities including overdispersion, random and clustered spatial patterns at a variety of intensities (Anderson et al. 1982; Lieberman et al. 1985; Taylor and Woiwod 1982; Condit et al. 2000). This work and the spatial patterns revealed here, along with our targeted model fitting, suggest that multiple mechanisms likely work in concert to produce emergent spatial patterns in communities of reef-building corals.

Spatial dispersion patterns: abiotic factors

A variety of abiotic factors can affect the distribution and spatial patterns of corals across the landscape. For example, the degree of fragmentation in branching corals has been shown to be positively related to the intensity and frequency of disturbance. Previous work has shown significant and complicated patterns of variation in the physical environment around Palmyra (Williams et al. 2013)

that may partially explain the observed high degree of variability in dispersion patterns for some of our coral groups. For instance, while corals of the free-living genus *Fungia* and branching species of *Acropora* were consistently clustered, they also displayed the highest variability in dispersion values. The observed clustering in *Fungia* may also be the result of large-scale physical factors such as the direction of predominant wave energy and currents that may transport these free-living corals to particular locations on the reef. The clustering of adults across the landscape may also be the result of larval preferences for, and availability of, suitable habitat (i.e., habitat filtering). If the distribution of suitable habitat is heterogeneous, or uniform, recruitment patterns should also be expected to be clustered.

Spatial dispersion patterns: biotic factors

Important differences in growth strategies may in part explain the observed levels of clustering. Many invertebrates, particularly colonial organisms such as corals, have the unique ability to grow almost without limit and sustain fluctuations in body size in response to stress (Jackson and Coates 1986; Sebens 1987). The ability of colonial organisms to tolerate stress via loss of individual clones without suffering total colony mortality allows corals to grow indeterminately (Jackson and Hughes 1985; Hughes et al. 1992) which is reflected in many corals through high rates of partial survival and regrowth following fragmentation (Hughes and Jackson 1980; Highsmith 1982; Furby et al. 2017). The formation of multiple daughter colonies from a single parent occurs through fission, fragmentation and budding (Highsmith 1982; Hughes and Connell 1987). Differences in these processes may produce fundamentally different spatial patterns as new colonies formed from fragmentation arise via skeletal fracturing and have some limited dispersal capabilities. In contrast, colonies formed via fission of tissues alone will necessarily be unable to disperse and may later fuse to reform a single colony following regrowth, resulting in necessarily more restricted spatial distributions.

Encrusting corals, particularly *Pavona varians*, *Porites superfusa*, and those in the genera *Favites* and *Montipora*, showed strong clustering with low levels of variation. These corals, and *Porites superfusa* in particular, have remarkable regenerative capabilities, with colony fragments readily surviving after fusion and new growth readily originating from these surviving fragments (Furby et al. 2017). Visual inspection of imagery also suggests that individuals from these genera are frequently highly fragmented via fission, likely producing the observed clustering. It is perhaps not surprising that there is repeated support for models of clustering (models 3 and 4) given that fission and regrowth of large coral colonies are typically constrained to areas of the colony's original footprint, namely the limestone previously accreted by the colony.

We also found moderate clustering in sub-massive *Pavona* and *Favia stelligera*. The distribution of sub-massive *Pavona* fit null clustering models, comparable to the patterns observed for the encrusting corals. In contrast, none of the null models consistently fit data for *Favia stelligera*, suggesting that the distribution of this species is structured by a complex collection of mechanisms. Interestingly, while both these species readily fragment via fission, fusion is more common in *Favia stelligera*.

The distributions of both branching and corymbose *Acropora* species were clustered, with the pattern consistent with models of both habitat filtering and biotic clustering mechanisms (Fig. 4). Many *Acropora* species have impressive regenerative capabilities and readily produce viable fragments (Highsmith 1982; Wallace 1985; Riegl and Piller 2001; Diaz-Pulido et al. 2009). Branching *Acropora* was strongly clustered, but the level of clustering was variable, perhaps reflecting plot-specific differences in habitat patterning. Levels of clustering in corymbose *Acropora* were lower and showed much less variability. Interestingly, as the distributions of both groups fit all the null spatial models tested here (except for the CSR model), the effects of habitat filtering may be equally important drivers of clustering patterns in addition to fragmentation. Another readily fragmenting group, *Lobophyllia*, which lives colonially but without tissue connections between adjacent polyps (Brickner et al. 2006), also showed high levels of clustering with moderate variability and was supported by both clustering null models. The spatial patterns reported here represent the first records for the majority of the central Pacific coral groups examined and are consistent with the hypothesis that fragmentation plays a key role in determining the spatial patterns of coral communities.

At the functional morphology level, the increase in clustering largely follows a gradient from determinate to indeterminate growth, i.e., from taxa known to grow more or less linearly to bounded maximum sizes, to taxa with fluid growth capabilities and without clear size limits, respectively (Highsmith 1982; Hughes 1987; Sebens 1987). Determinate growth in corals is frequently associated with corymbose and plating taxa with small maximum size, high growth rates and fecundity and low stress tolerance (Szmant 1986). The lower levels of clustering found in these groups (e.g., *Pocillopora*, *Montipora*) are likely the result of the relatively lower survivorship and regenerative capabilities of both adult colonies and fragments. This is contrasted with indeterminate growth in corals, which is generally associated with slower growing, stress-tolerant sub-massive and massive forms (Highsmith 1982; Szmant

1986; Hughes et al. 1992). Fragmentation and regrowth are known functions of indeterminate growth and have been positively linked to increasing size and inherent morphological characteristics in massive and other corals (Hughes and Connell 1987; DeVantier and Endean 1989; Pisapia and Pratchett 2014).

At the other extreme, free-living corals exhibit unique growth traits that are associated with indeterminism, likely contributing to their high degree of clustering. Remnant tissue in injured adult colonies, and even seemingly dead ones, has the potential to produce large numbers of buds (Kramarsky-Winter and Loya 1996). Despite potentially limited facultative dispersal and habitat selectivity, this movement is highly spatially constrained due to habitat effects. The results of the model-fitting procedure strongly support the conclusion that budding processes have produced the highly clustered patterns observed here (Fig. 4). The final group considered, encrusting corals, showed the second highest median level of clustering. While generally considered less stress tolerant, some encrusting corals have a remarkable ability to undergo fission and regrowth (Furby et al. 2017), likely leading to the high level of clustering found here. As some coral taxa have a mix of these traits, the patterns observed here are likely the result of interactions among traits.

Dispersal in sessile organisms such as plants, algae, fungi, bryozoans and reef-building corals occurs via a limited number of processes. Though some free-living corals have limited facultative dispersal (Chadwick 1988), generally, adult coral dispersal will only occur following dislodgement or fragmentation as a result of biophysical forcing (e.g., storms, waves). Consequently, the dispersive pattern of early life stages (e.g., larvae) will drive recruitment patterns and ultimately the spatial structure of sessile communities (Hubbell 1979; Condit et al. 2000). The reproductive strategies of corals can largely be categorized as spawning or brooding. Brooding corals produce fully competent larvae that can settle and metamorphose in the immediate vicinity of parent colonies following release of planulae (Carlon and Olson 1993). In contrast, gametes released via broadcast spawning are released into the water column where they are subject to mixing and must be transported to settlement locations. Variation in these reproductive modes may therefore be expected to lead to differences in the spatial distributions of adult corals. Previous evidence has shown large-scale spatial structuring of coral communities related to reproductive mode (Stimson 1978), but inter-colony spatial variation due to differences in reproductive mode has seldom been explicitly considered (but see Carlon and Olson 1993). Here we found the brooding coral, *Stylophora pistillata*, exhibited moderate levels of clustering, while broadcasting corals, *Pocillopora* in particular, showed levels of dispersion much closer to randomness, perhaps resulting from the differences outlined above.

Spatial dispersion patterns: density dependence

Several of the functional and taxonomic groups showed significant positive relationships between plot-specific VMR and colony abundance (Table 3). These relationships may arise from fundamental processes of reproduction, aggregation and repulsion. Taylor's law (Taylor 1961; Taylor and Woiwod 1982) asserts that log–log relationships between variance and mean abundance can be expected to have positive slopes of 1–2, which is equivalent to slopes between 0 and 1 when relating VMR and mean (ESM Methods 2). We found significant relationships with slopes ranging from 0.225 to 0.650 for taxonomic groups and from 0.411 to 0.761 for functional morphology groups (Table 3). Moreover, while only a handful of the taxonomic and functional groups had significant VMR–abundance relationships, the general trend of positive relationships across all taxonomic groups occurred significantly more frequently than expected by chance alone (21 of 23 groups, binomial test, $p < 0.01$), following the predictions of Taylor's law. This relationship, however, was not significant at the functional morphology level (three of eight groups, binomial test, $p = 0.07$), suggesting that species-specific traits may be an important determinant of density-dependent processes.

The value of these slopes should correlate positively with fragmentation/reproduction rates. However, inferring relationships between ecological processes should be treated with caution (Anderson et al. 1982; Routledge and Swartz 1991). Interestingly, species with high reproduction/fragmentation rates living in heterogeneous environments can exhibit steeper slopes than species with a lower reproduction/fragmentation rate in more homogeneous environments (Anderson et al. 1982). Here, the strongest relationship was found for *Fungia* (Table 3), perhaps reflecting the comparatively high reproductive rates and constraints imposed on the free-living morphology in more topographically and hydrodynamically heterogeneous areas. For other groups, the strength of relationship between the level of clustering and abundance appears to arise from the capacity of a group to use fragmentation as a survival/reproductive mechanism, as seen in the significant positive relationships found for encrusting *Porites superfusa* and *Montipora*. We also saw a significant relationship for *Pocillopora,* which dominates juvenile coral (< 9 cm^2) abundances across the majority of our plots. This suggests that interactions between habitat heterogeneity and reproduction may be contributing strongly to the results found here.

Acknowledgements This work was made possible through funding provided by the Gordon and Betty Moore Foundation, Grant #3420, and the UC San Diego Frontiers of Innovations Scholarship Program. We are grateful to Gideon Butler, Sho Kodera and Tayler Fewell who contributed to image digitization. This is Palmyra Atoll Research Consortium contribution ## PARC-0125. Thank you to The Nature Conservancy and the Palmyra Atoll Research Consortium for logistical support and the United States Fish Wildlife Service for special use permit # 12533-13025 and access to the refuge.

References

Anderson RM, Gordon DM, Crawley MJ, Hassell MP (1982) Variability in the abundance of animal and plant species. Nature 296:245–248

Baddeley A, Rubak E, Turner R (2015) Spatial point patterns: methodology and applications with R. Chapman & Hall/CRC Press, Boca Raton

Bak R, Engel M (1979) Distribution, abundance and survival of juvenile hermatypic corals (Scleractinia) and the importance of life history strategies in the parent coral community. Mar Biol 54:341–352

Bak R, Termaat R, Dekker R (1982) Complexity of coral interactions: influence of time, location of interaction and epifauna. Mar Biol 69:215–222

Bellwood DR, Hughes TP, Folke C, Nystrom M (2004) Confronting the coral reef crisis. Nature 429:827–833

Bormann FH, Likens G (2012) Pattern and process in a forested ecosystem: disturbance, development and the steady state based on the Hubbard Brook ecosystem study. Springer-Verlag, New York

Bradbury RR, Young PP (1981) The effects of a major forcing function, wave energy, on a coral reef ecosystem. Mar Ecol Prog Ser 5:229–241

Bradbury R, Young P (1983) Coral interactions and community structure: an analysis of spatial pattern. Mar Ecol Prog Ser 11:265–271

Brickner I, Oren U, Frank U, Loya Y (2006) Energy integration between the solitary polyps of the clonal coral *Lobophyllia corymbosa*. J Exp Biol 209:1690–1695

Carlon DB, Olson RR (1993) Larval dispersal distance as an explanation for adult spatial pattern in two Caribbean reef corals. J Exp Mar Bio Ecol 173:247–263

Chadwick NE (1988) Competition and locomotion in a free-living fungiid coral. J Exp Mar Bio Ecol 123:189–200

Condit R, Ashton PS, Baker P, Bunyavejchewin S, Gunatilleke S, Gunatilleke N, Hubbell SP, Foster RB, Itoh A, LaFrankie JV, Lee HS, Losos E, Manokaran N, Sukumar R, Yamakura T (2000) Spatial patterns in the distribution of tropical tree species. Science 288:1414–1418

Connell JH (1978) Diversity in tropical rain forests and coral reefs. Science 199:1302–1310

Connell JH (1985) The consequences of variation in initial settlement vs. post-settlement mortality in rocky intertidal communities. J Exp Mar Bio Ecol 93:11–45

Dale MRT (1999) Spatial pattern analysis in plant ecology. Ecology 88:366–370

Dale MRT, Dixon P, Fortin M-J, Legendre P, Myers DE, Rosenberg MS (2002) Conceptual and mathematical relationships among methods for spatial analysis. Ecography 25:558–577

Dana TF (1976) Reef-coral dispersion patterns and environmental variables on a Caribbean coral reef. Bull Mar Sci 26:1–13

Deignan L, Pawlik J (2015) Perilous proximity: does the Janzen-Connell hypothesis explain the distribution of giant barrel sponges on a Florida coral reef? Coral Reefs 34:561–567

DeVantier L, Endean R (1989) Observations of colony fission following ledge formation in massive reef corals of the genus *Porites*. Mar Ecol Prog Ser 58:191–195

Diaz-Pulido G, McCook LJ, Dove S, Berkelmans R, Roff G, Kline DI, Weeks S, Evans RD, Williamson DH, Hoegh-Guldberg O (2009) Doom and boom on a resilient reef: climate change, algal overgrowth and coral recovery. PLoS ONE 4:e5239

Edmunds PJ (2015) A quarter-century demographic analysis of the Caribbean coral, *Orbicella annularis*, and projections of population size over the next century. Limnol Oceanogr 60:840–855

Furby KA, Smith JE, Sandin SA (2017) *Porites superfusa* mortality and recovery from a bleaching event at Palmyra Atoll, USA. Peer J 1:e3204

Goreau TF (1959) The ecology of Jamaican coral reefs I. Species composition and zonation. Ecology 40:67–90

Gracias NR, Van Der Zwaan S, Bernardino A, Santos-Victor J (2003) Mosaic-based navigation for autonomous underwater vehicles. IEEE J Oceanic Eng 28:609–624

Harms KE, Wright SJ, Calderon O, Hernandez A, Herre EA (2000) Pervasive density-dependent recruitment enhances seedling diversity in a tropical forest. Nature 404:493–495

Highsmith RC (1982) Reproduction by fragmentation in corals. Mar Ecol Prog Ser 7:207–226

Highsmith RC, Riggs AC, D'Antonio CM (1980) Survival of hurricane-generated coral fragments and a disturbance model of reef calcification/growth rates. Oecologia 46:322–329

Hubbell SP (1979) Tree dispersion, abundance, and diversity in a tropical dry forest. Science 203:1299–1309

Hubbell SP, Foster RB (1992) Short-term dynamics of a neotropical forest: why ecological research matters to tropical conservation and management. Oikos 63:48–61

Hughes R (1987) The functional ecology of clonal animals. Funct Ecol 1:63–69

Hughes TP (1984) Population dynamics based on individual size rather than age: a general model with a reef coral example. Am Nat 123:778–795

Hughes T, Jackson J (1980) Do corals lie about their age? Some demographic consequences of partial mortality, fission, and fusion. Science 209:713–715

Hughes TP, Connell JH (1987) Population dynamics based on size or age? A reef-coral analysis. Am Nat 129:818–829

Hughes TP, Tanner JE (2000) Recruitment failure, life histories, and long-term decline of Caribbean corals. Ecology 81:2250–2263

Hughes TP, Ayre D, Connell JH (1992) The evolutionary ecology of corals. Trends Ecol Evol 7:292–295

Hutchinson GE (1953) The concept of pattern in ecology. Proceedings of the Academy of Natural Sciences of Philadelphia 105:1–12

Jackson JBC, Hughes TP (1985) Adaptive strategies of coral-reef invertebrates: coral-reef environments that are regularly disturbed by storms and by predation often favor the very organisms most susceptible to damage by these processes. Am Sci 73:265–274

Jackson JBC, Coates AG (1986) Life cycles and evolution of clonal (modular) animals. Proc R Soc Lond B Biol Sci 313:7–22

Janzen DH (1970) Herbivores and the number of tree species in tropical forests. Am Nat 104:501–528

Jolles AE, Sullivan P, Alker AP, Harvell CD (2002) Disease transmission of aspergillosis in sea fans: inferring process from spatial pattern. Ecology 83:2373–2378

Karlson RH, Cornell HV, Hughes TP (2007) Aggregation influences coral species richness at multiple spatial scales. Ecology 88:170–177

Kenyon JC, Maragos JE, Cooper S (2010) Characterization of coral communities at Rose Atoll, American Samoa. Atoll Res Bull 586:1–28

Kramarsky-Winter E, Loya Y (1996) Regeneration versus budding in fungiid corals: a trade-off. Mar Ecol Prog Ser 134:179–185

Lewis JB (1970) Spatial distribution and pattern of some Atlantic reef corals. Nature 227:1158–1159

Lieberman D, Lieberman M, Peralta R, Hartshorn GS (1985) Mortality patterns and stand turnover rates in a wet tropical forest in Costa Rica. J Ecol 73:915–924

Lirman D, Gracias NR, Gintert BE, Gleason ACR, Reid RP, Negahdaripour S, Kramer P (2007) Development and application of a video-mosaic survey technology to document the status of coral reef communities. Environ Monit Assess 125:59–73

Marhaver K, Vermeij M, Rohwer F, Sandin S (2013) Janzen-Connell effects in a broadcast-spawning Caribbean coral: distance-dependent survival of larvae and settlers. Ecology 94:146–160

Newman MJH, Paredes GA, Sala E, Jackson JBC (2006) Structure of Caribbean coral reef communities across a large gradient of fish biomass. Ecol Lett 9:1216–1227

Pisapia C, Pratchett MS (2014) Spatial variation in background mortality among dominant coral taxa on Australia's Great Barrier Reef. PLoS ONE 9:e100969

R Core Team (2016) R: a language and environment for statistical computing. R Foundation for Statistical Computing, Vienna

Reichelt R, Bradbury R (1984) Spatial patterns in coral reef benthos: multiscale analysis of sites from three oceans. Mar Ecol Prog Ser 17:251–257

Riegl B, Piller W (2001) Cryptic tissues inside *Acropora* frameworks (Indonesia): a mechanism to enhance tissue survival in hard times while also increasing framework density. Coral Reefs 20:67–68

Rietkerk M, van de Koppel J (2008) Regular pattern formation in real ecosystems. Trends Ecol Evol 23:169–175

Roff G, Bejarano S, Bozec Y-M, Nugues M, Steneck RS, Mumby PJ (2014) *Porites* and the phoenix effect: unprecedented recovery after a mass coral bleaching event at Rangiroa Atoll, French Polynesia. Mar Biol 161:1385–1393

Routledge RD, Swartz TB (1991) Taylor's power law re-examined. Oikos 60:107–112

Sandin SA, Smith JE, DeMartini EE, Dinsdale EA, Donner SD, Friedlander AM, Konotchick T, Malay M, Maragos JE, Obura D (2008) Baselines and degradation of coral reefs in the northern Line Islands. PLoS ONE 3:e1548

Sebens KP (1987) The ecology of indeterminate growth in animals. Annu Rev Ecol Evol Syst 18:371–407

Smith JE, Brainard R, Carter A, Grillo S, Edwards C, Harris J, Lewis L, Obura D, Rohwer F, Sala E, Vroom PS, Sandin S (2016) Re-evaluating the health of coral reef communities: baselines and evidence for human impacts across the central Pacific. Proc R Soc Lond B Biol Sci 283:20151985

Stimson J (1974) An analysis of the pattern of dispersion of the hermatypic coral *Pocillopora meandrina* var. *nobilis* Verril. Ecology: 445–449

Stimson JS (1978) Mode and timing of reproduction in some common hermatypic corals of Hawaii and Enewetak. Mar Biol 48:173–184

Szmant AM (1986) Reproductive ecology of Caribbean reef corals. Coral Reefs 5:43–53

Taylor L (1961) Aggregation, variance and the mean. Nature 189:732–735

Taylor L, Woiwod I (1982) Comparative synoptic dynamics. I. Relationships between inter- and intra-specific spatial and temporal variance/mean population parameters. J Anim Ecol 51:879–906

Turner MG (1989) Landscape ecology: the effect of pattern on process. Annu Rev Ecol Evol Syst 20:171–197

Velázquez E, Martínez I, Getzin S, Moloney KA, Wiegand T (2016) An evaluation of the state of spatial point pattern analysis in ecology. Ecography 39:1042–1055

Wallace CC (1985) Reproduction, recruitment and fragmentation in nine sympatric species of the coral genus *Acropora*. Mar Biol 88:217–233

Williams GJ, Smith JE, Conklin EJ, Gove JM, Sala E, Sandin SA (2013) Benthic communities at two remote Pacific coral reefs: effects of reef habitat, depth, and wave energy gradients on spatial patterns. Peer J 1:e81

Wu J (2013) Landscape sustainability science: ecosystem services and human well-being in changing landscapes. Landsc Ecol 28:999–1023

Zvuloni A, Artzy-Randrup Y, Stone L, Kramarsky-Winter E, Barkan R, Loya Y (2009) Spatio-temporal transmission patterns of black-band disease in a coral community. PLoS ONE 4:e4993